

Supporting Information for

**Bubble-Propelled Micro-/Nanomotors of Variable Size by
Regulating Surface Microstructure of Partial Coating Shell Pt**

Jiaxin Li¹, Xiangxiang Zhai¹, Zili Yang¹, Ziyi Pei¹, Ming Luo^{1}, and Jianguo Guan^{1,2*}*

1. State Key Laboratory of Advanced Technology for Materials Synthesis and Processing, International School of Materials Science and Engineering, Wuhan University of Technology, Wuhan 430070, China.
2. Wuhan Institute of Photochemistry and Technology, 7 North Bingang Road, Wuhan, Hubei 430083, China.

*Address correspondence to luoming_2016@whut.edu.cn (M. Luo), guanjq@whut.edu.cn (J. Guan)

Table of Contents

1. Supporting figures.....S22

Figure S1. SEM and TEM images of 1- μm PS microspheres.

Figure S2. SEM and TEM images of 1- μm PS@PDA core-shell microstructures.

Figure S3. Fourier transform infrared (FTIR) spectra of PS@PDA core-shell microstructures (up) and PS microspheres (down).

Figure S4. SEM and TEM images of 1- μm PS-PS@PDA eccentric particles.

Figure S5. SEM and TEM images of 500-nm PS microspheres.

Figure S6. SEM and TEM images of 500-nm PS@PDA core-shell microstructures.

Figure S7. SEM and TEM images of 500-nm PS-PS@PDA eccentric particles.

Figure S8. SEM and TEM images of 500-nm PEMNMs.

Figure S9. SEM and TEM images of 200-nm PS microspheres.

Figure S10. SEM and TEM images of 200-nm PS@PDA core-shell microstructures.

Figure S11. SEM and TEM images of 200-nm PS-PS@PDA eccentric particles.

Figure S12. SEM and TEM images of 200-nm PEMNMs.

Figure S13. The time-lapse images show the interaction behavior between 1- μm PEMNM and tracer particles in H_2O_2 aqueous solutions.

Figure S14. Differentiation of the propulsion mechanism of PEMNM.

Figure S15. The motion behavior of 1- μm PEMNM in H_2O_2 aqueous solution containing different NaCl concentration.

Figure S16. The migration speed of 1- μm PEMNM in H_2O_2 aqueous solution (10% v/v).

Figure S17. Typical trajectories of 1- μm PEMNMs with low surface coverage of PtNPs in H_2O_2 aqueous solutions.

Figure S18. The Pt content of 1- μm PEMNMs with different surface coverage of PtNPs.

Figure S19. Amount of oxygen produced by 1- μm PEMNMs with different surface coverage of Pt nanoparticles immersed in H_2O_2 aqueous solutions.

Figure S20. Typical trajectories of 1- μm PEMNMs with high surface coverage of PtNPs in H_2O_2 aqueous solutions.

Figure S21. Typical trajectories of 500-nm PEMNMs in 15% H_2O_2 aqueous solutions.

Figure S22. Typical trajectories of 200-nm PEMNMs in 20% H_2O_2 aqueous solutions.

2. Supporting tables.....S23

Table S1. Summary of the bubble-propelled MNMs

3. Supporting videos

Video S1. Motion behavior of the 1- μm PEMNMs in H_2O_2 aqueous solutions (3% v/v)

Video S2. Motion behavior of the 1- μm PEMNMs in H_2O_2 aqueous solutions (10% v/v)

Video S3. The interaction behavior between 1- μm PEMNM and tracer particles in 3% v/v H_2O_2 aqueous solutions.

Video S4. Motion behavior of the 500-nm PEMNMs in H_2O_2 aqueous solutions (15% v/v)

Video S5. Motion behavior of the 200-nm PEMNMs in H_2O_2 aqueous solutions (20% v/v)

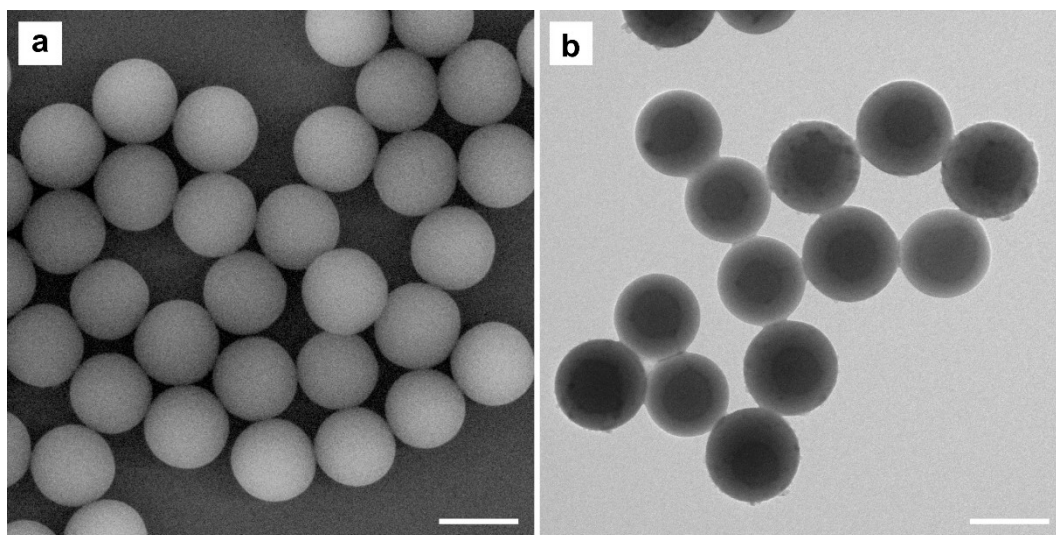


Figure S1. SEM (a) and TEM (b) images of 1- μm PS microspheres. Scale bars: 1 μm .

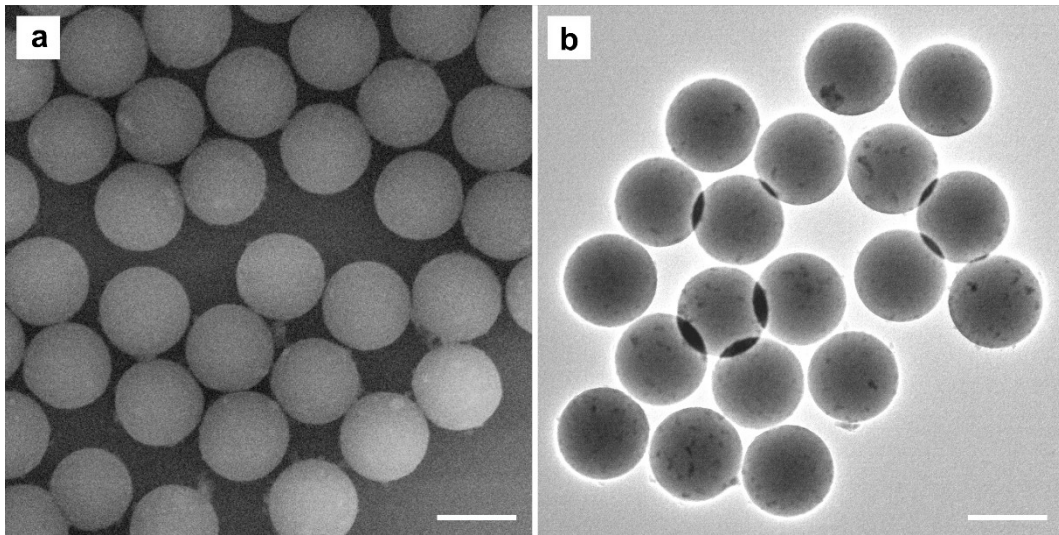


Figure S2. SEM (a) and TEM (b) images of 1- μm PS@PDA core-shell microstructures. Scale bars: 1 μm .

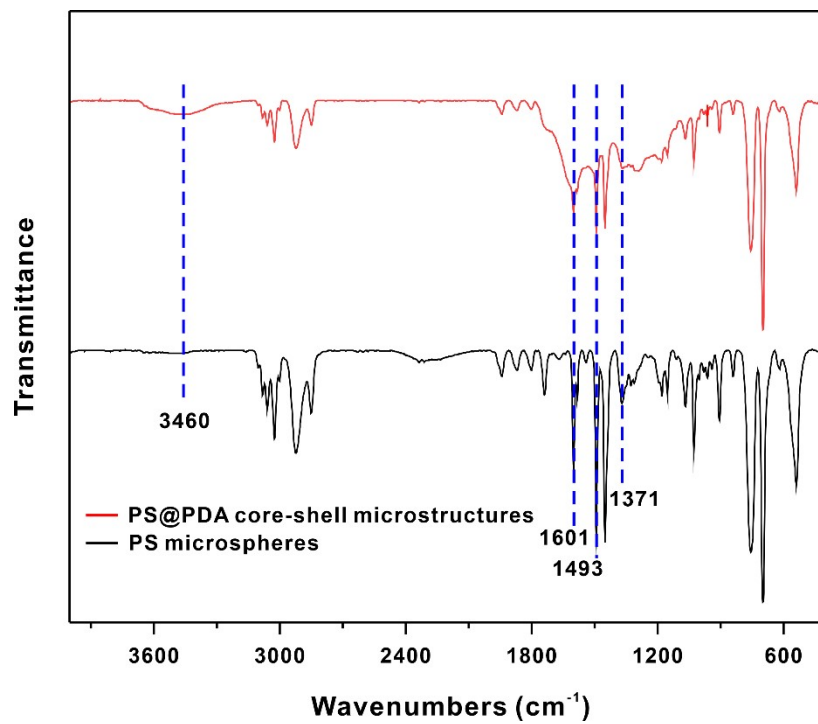


Figure S3. Fourier transform infrared (FTIR) spectra of PS spheres and PS@PDA core-shell microstructures.

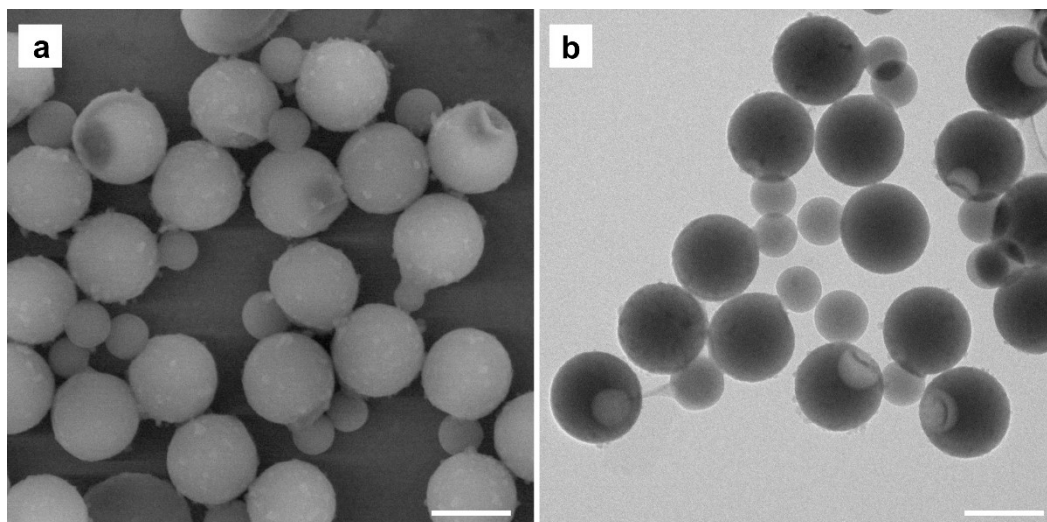


Figure S4. SEM (a) and TEM (b) images of 1- μm PS-PS@PDA eccentric particles. Scale bars: 1 μm .

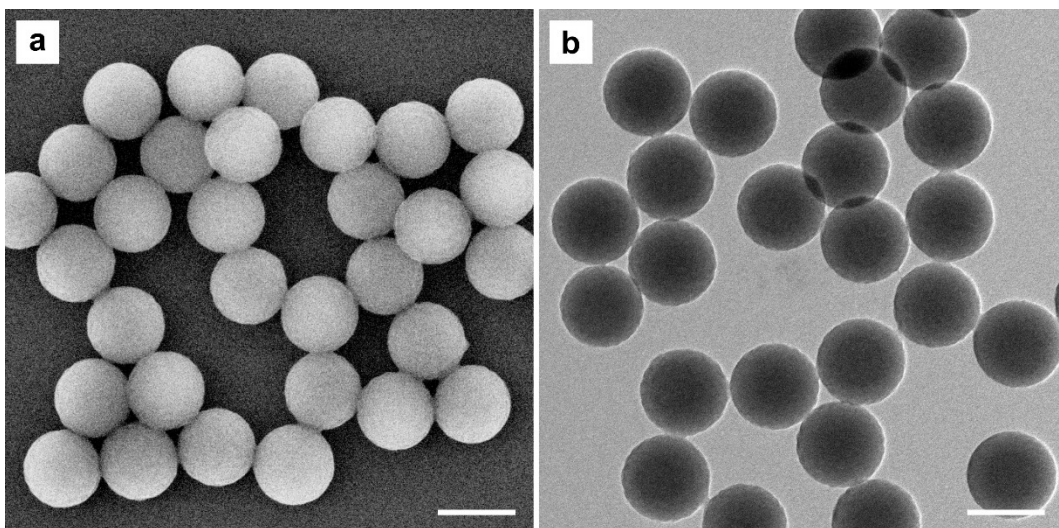


Figure S5. SEM (a) and TEM (b) images of 500-nm PS microspheres. Scale bars: 500 nm.

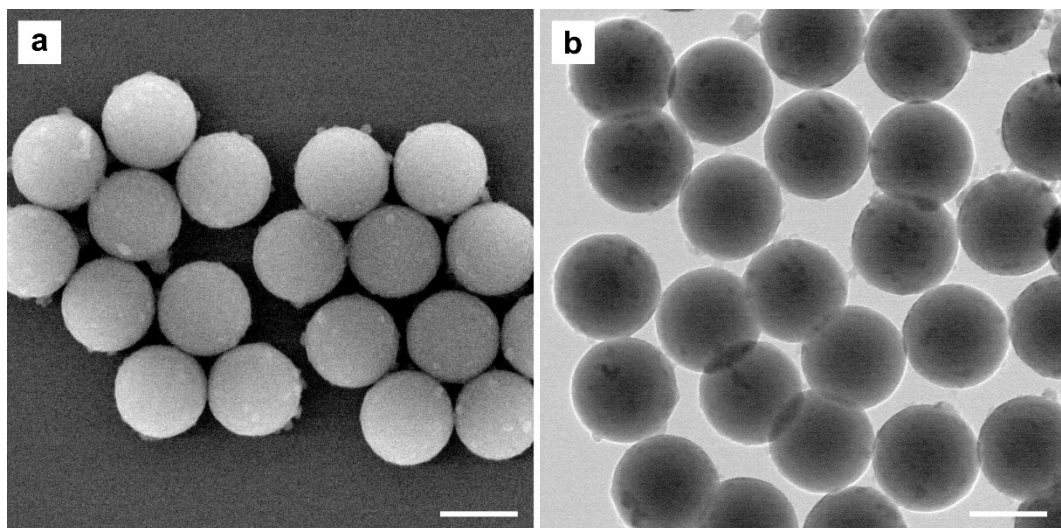


Figure S6. SEM (a) and TEM (b) images of 500-nm PS@PDA core-shell nanostructures. Scale bars: 500 nm.

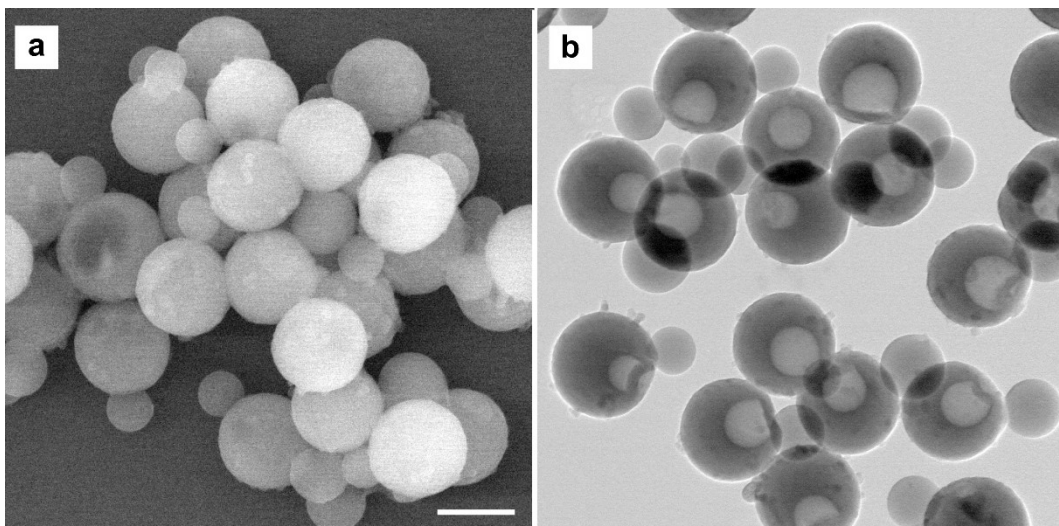


Figure S7. SEM (a) and TEM (b) images of 500-nm PS-PS@PDA eccentric particles Scale bars: 500 nm.

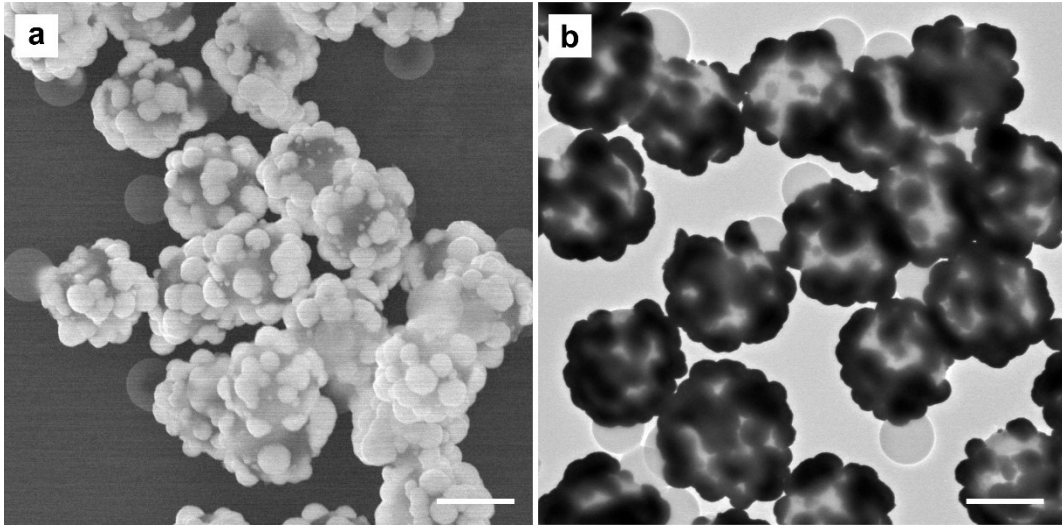


Figure S8. SEM (a) and TEM (b) images of 500-nm PEMNM structures. Scale bars: 500 nm.

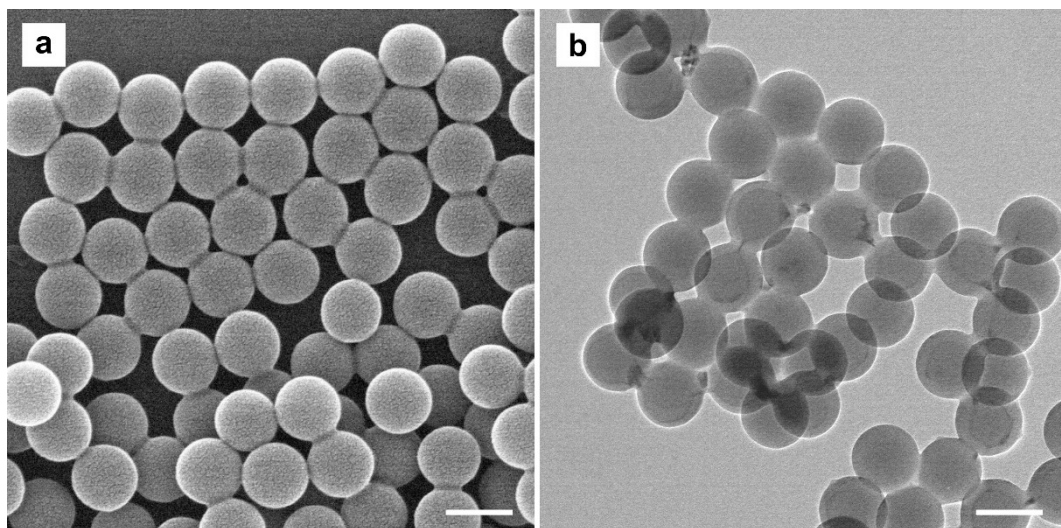


Figure S9. SEM (a) and TEM (b) images of 200-nm PS microspheres. Scale bars: 200 nm.

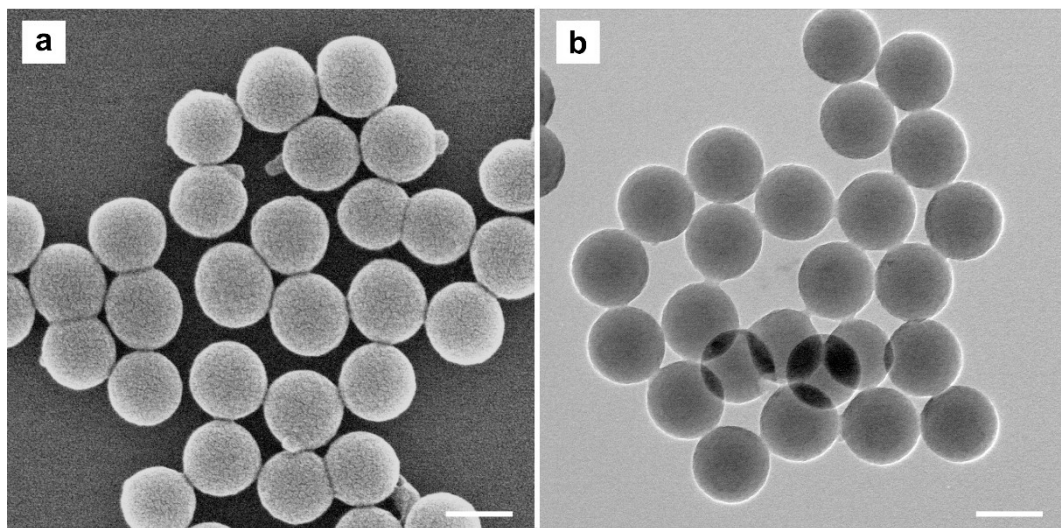


Figure S10. SEM (a) and TEM (b) images of 200-nm PS@PDA core-shell microstructures. Scale bars: 200 nm.

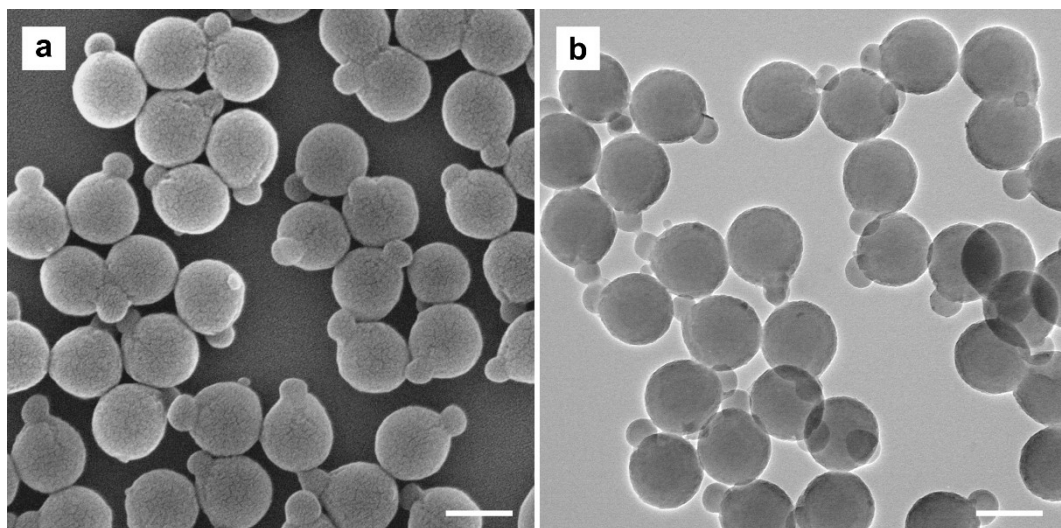


Figure S11. SEM (a) and TEM (b) images of 200- μm PS-PS@PDA eccentric particles. Scale bars: 200 nm.

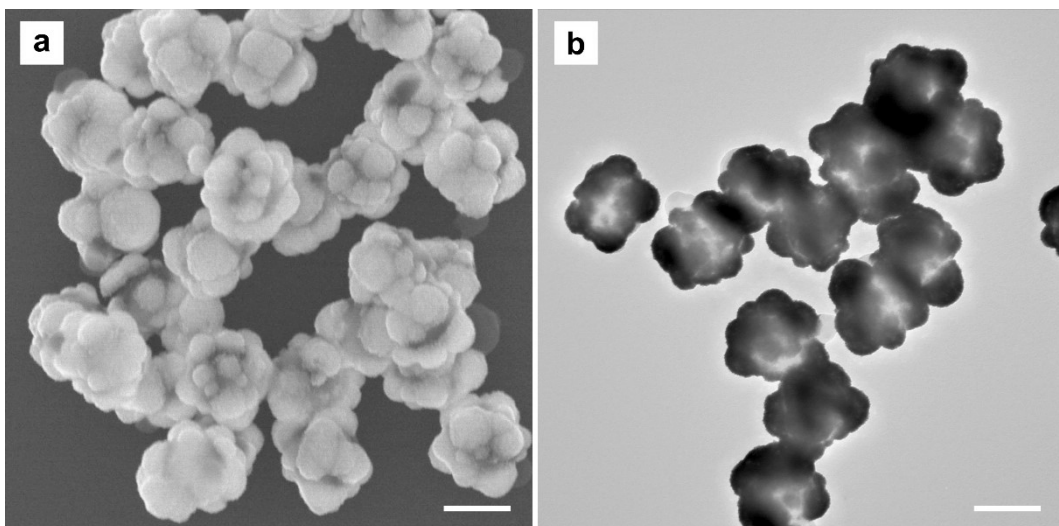


Figure S12. SEM (a) and TEM (b) images of 200-nm PEMNM structures. Scale bars: 200 nm.

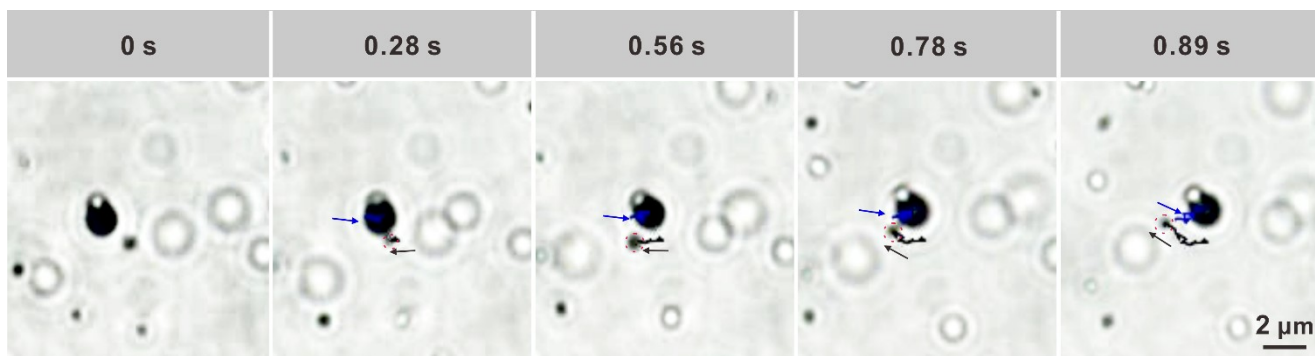


Figure S13. Verification of the propulsion mechanism of 1- μm PEMNM by the tracer particle-assisted experiments. The time-lapse images showed the interaction behavior between 1- μm PEMNM and tracer particles (500-nm SiO_2 nanoparticles) in H_2O_2 aqueous solutions (3% v/v). The images were obtained from the [Video S3](#).

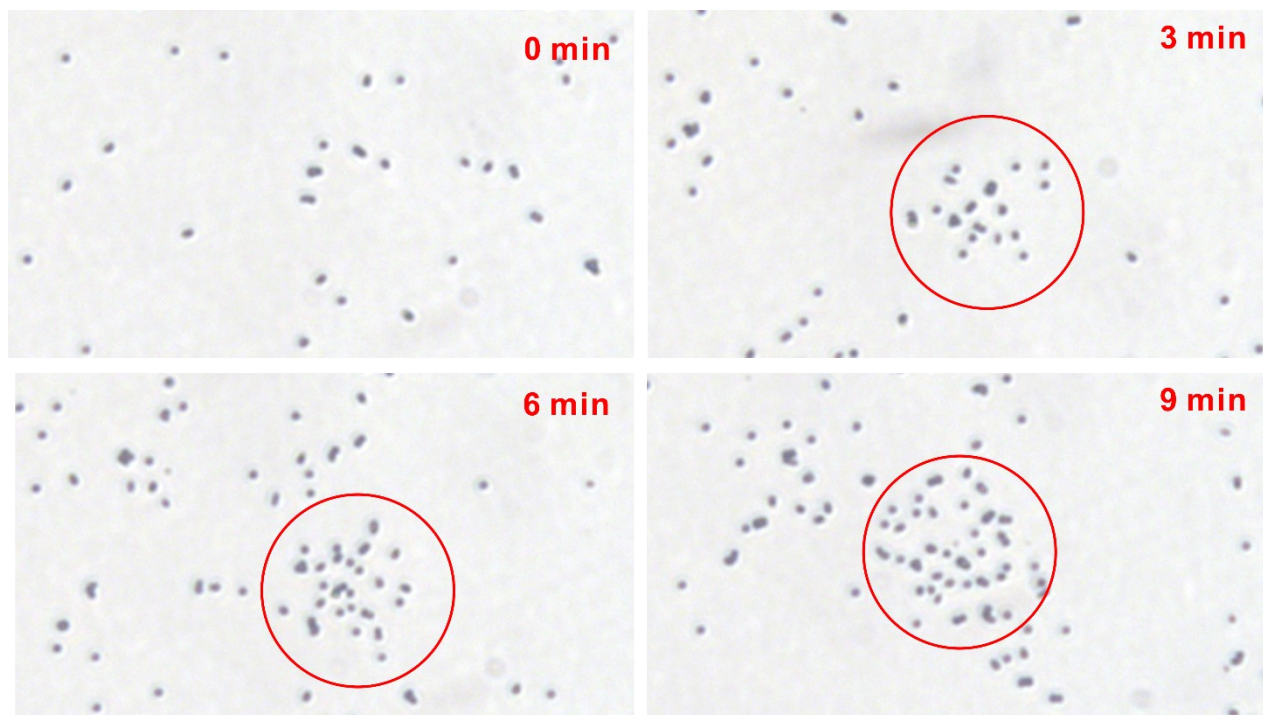


Figure S14. Differentiation of the propulsion mechanism of PEMNM by the method reported by Wang and co-workers. The time-lapse images show the interaction behavior between 1- μm PEMNM in H_2O_2 aqueous solutions (3% v/v).

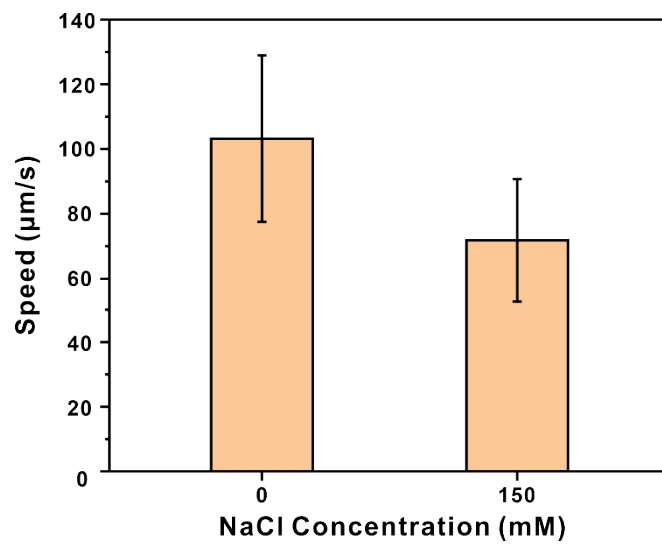


Figure S15. The motion behavior of 1-µm PEMNM when immersed in H₂O₂ aqueous solution (10% v/v) containing different NaCl concentration.

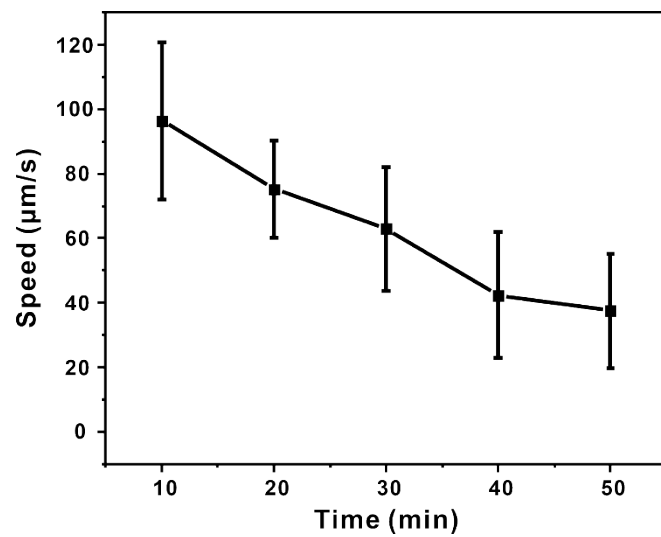


Figure S16. The migration speed of 1- μm PEMNM within 50 minutes when immersed in H_2O_2 aqueous solution (10% v/v).

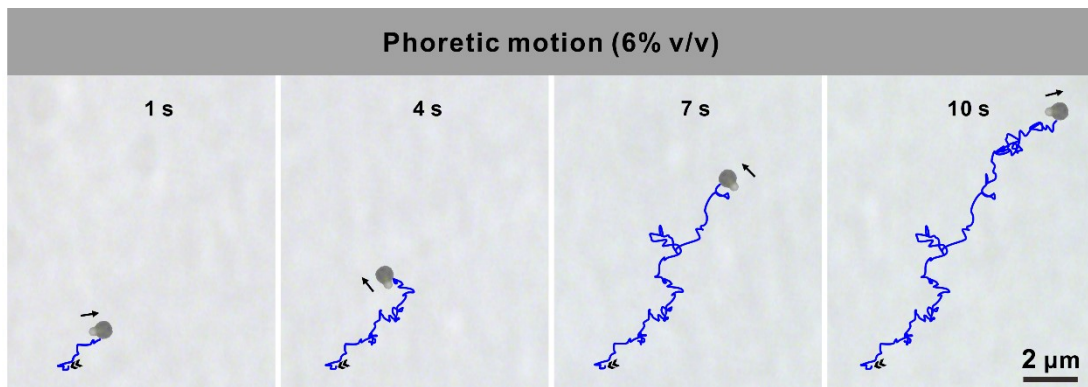


Figure S17. Typical trajectories of 1- μm PEMNMs with low surface coverage of PtNPs in H_2O_2 aqueous solution (6% v/v).

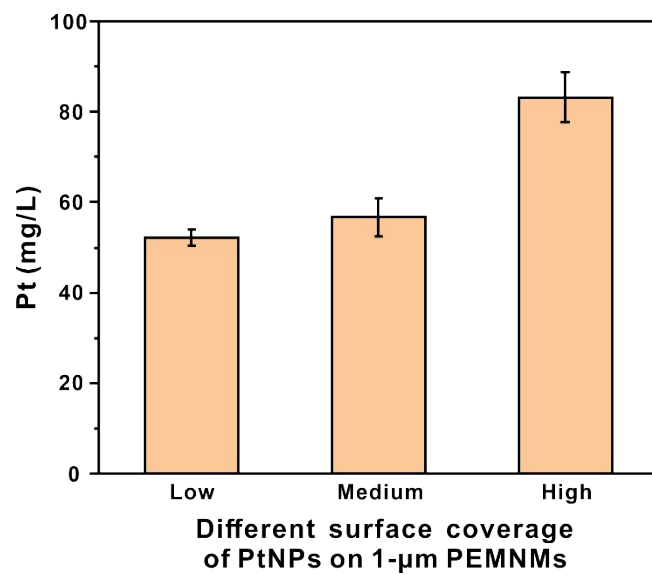


Figure S18. The Pt content of 1- μ m PEMNMs with different surface coverage of PtNPs. The number of motor is 2.28×10^8 .

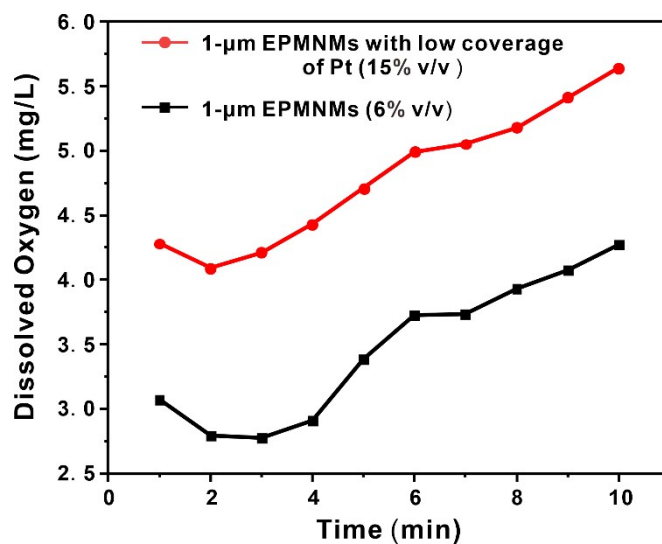


Figure S19. Amount of oxygen produced by 1-µm PEMNMs with different surface coverage of Pt nanoparticles immersed in H₂O₂ aqueous solutions.

Experimental section: In briefly, the same amount of 1-µm PEMNMs with different surface coverage of Pt nanoparticles was added into 5 mL of H₂O₂ aqueous solution. The produced oxygen was measured by a dissolved oxygen test instrument.

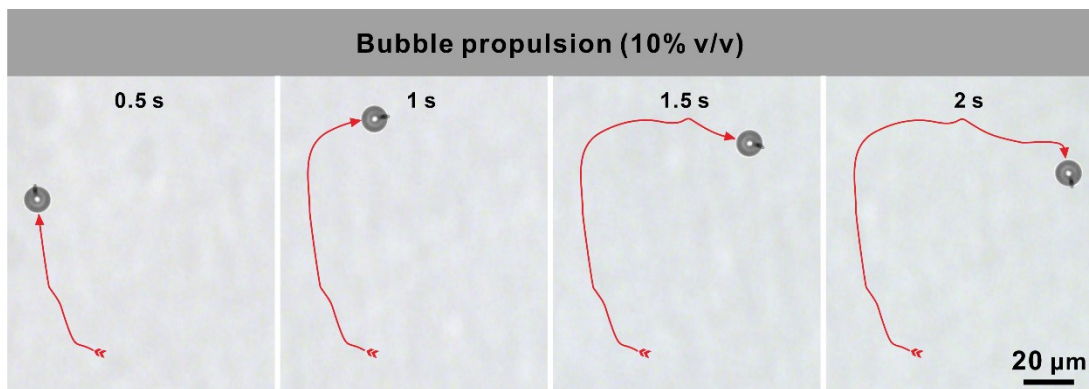


Figure S20. Typical trajectories of 1- μm PEMNMs with high surface coverage of PtNPs in H_2O_2 aqueous solution (10% v/v).

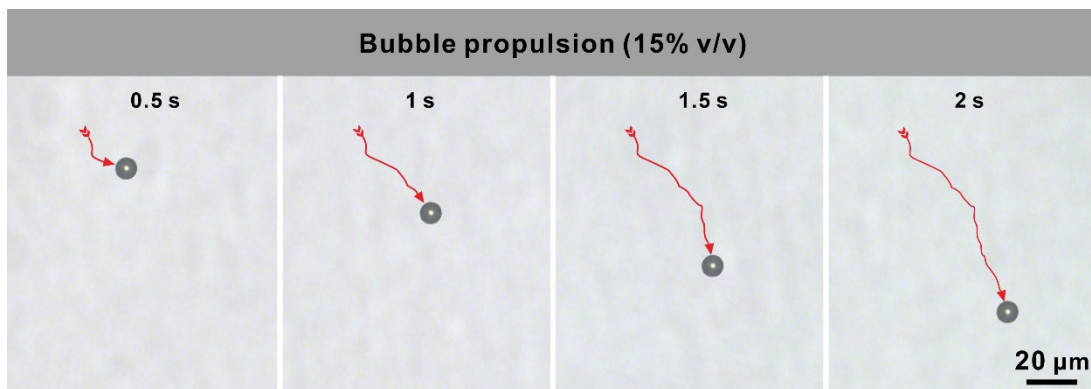


Figure S21. Typical trajectories of 500-nm PEMNMs in 15% v/v H₂O₂ aqueous solution. The images were obtained from the

[Video S4](#).

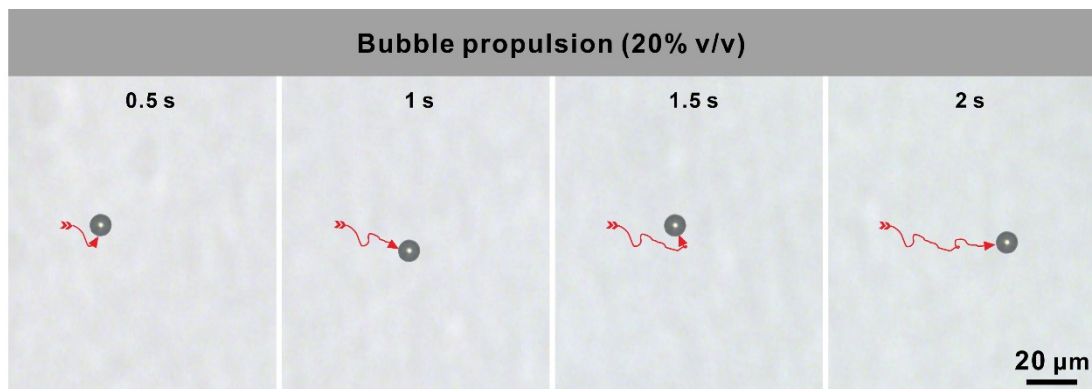


Figure S22. Typical trajectories of 200-nm PEMNMs in 20% v/v H₂O₂ aqueous solution. The images were obtained from the

[Video S5](#).

Table S1. Summary of the bubble-propelled MNMs.

| Micro-/Nanomotors | Morphology | Size | Fuel | Fabrication Technique | Application | Reference |
|---|-----------------|--|-------------------------------|----------------------------|--|---|
| Magnesium (Mg)/Platinum (Pt) Janus Micromotors | Janus Particles | ~20 μm (Diameter) (SEM) | Water | Physical Vapor Deposition | - | <i>Angew. Chem. Int. Ed.</i> , 2013 , 52, 7208–7212. |
| Hydrogen-Powered Microswimmers (HPMs) | Janus Particles | ~24 μm (Diameter) (SEM) | Water | Physical Vapor Deposition | ROS and inflammation scavenging | <i>Adv. Funct. Mater.</i> , 2021 , 31, 2009475. |
| Mg-Based Micromotors | Janus Particles | 23 \pm 5 μm (Diameter) (SEM) | Water | Physical Vapor Deposition | Therapy of rheumatoid arthritis | <i>Nano Lett.</i> , 2021 , 21, 1982–1991. |
| Enteric Mg Micromotors | Tubular | ~23.2 μm (Length) (SEM) | Water | Template Electrodeposition | Site-specific gastrointestinal delivery | <i>ACS Nano</i> , 2016 , 10, 9536–9542. |
| Aluminum (Al)-Gallium (Ga)/Titanium (Ti) Micromotor | Janus Particles | ~20 μm (Diameter) (SEM) | Water | Physical Vapor Deposition | - | <i>ACS Nano</i> , 2012 , 6, 8432–8438. |
| Multi-Response Biocompatible Janus Micromotor | Janus Particles | ~25 μm (Diameter) (SEM) | Water | Physical Vapor Deposition | Medical imaging | <i>Appl. Mater. Today.</i> , 2021 , 23, 101026. |
| Mg-TiO ₂ micromotor | Janus Particles | 20–25 μm (Diameter) (SEM) | Water | Physical Vapor Deposition | - | <i>Research</i> , 2020 , 2020, 7823615. |
| Zinc (Zn) / Iron (Fe) Janus Micromotors | Janus Particles | ~20 μm (Diameter) (SEM) | Acid | Physical Vapor Deposition | - | <i>ACS Nano</i> , 2016 , 10, 10389–10396. |
| Polyaniline (PANI)/Zn Micromotors | Tubular | ~0.35 μm (front inner Diameter) ~1.2 μm (outer layer Diameter) | Acid | Template Electrodeposition | Pick-up, transport, and release of cargoes | <i>J. Am. Chem. Soc.</i> , 2012 , 134, 897–900. |
| Zerovalent-Iron (ZVI)/Pt Janus Micromotors | Janus Particles | ~10 μm (Length) (SEM) | H ₂ O ₂ | Physical Vapor Deposition | Removal of 2,4-dinitrotoluene and Rhodamine 6G | <i>Small</i> , 2015 , 11, 499–506. |
| MOF-Integrated Photocatalytic Micromotors. | Janus Particles | ~60 μm (Diameter) (SEM) | H ₂ O ₂ | Colloidal Chemistry Method | Degradation of organic contaminant Rhodamine B | <i>ACS Appl. Mater. Interfaces</i> , 2020 , 12, 35120–35131. |
| Pt Micro/Nanomotors | Tubular | 0.23 μm to 4.74 μm (Diameter) 2.25 μm to 17.25 μm (Length) (SEM) | H ₂ O ₂ | Template Electrodeposition | - | <i>ACS Nano</i> , 2016 , 10, 5041–5050. |
| Tubular Catalytic Micromotors | Tubular | 10 μm (Diameter) 50 μm (Length) (SEM) | H ₂ O ₂ | Template Electrodeposition | - | <i>Small</i> , 2021 , 17, 2006449 |

| | | | | | | |
|---|-------------------|---|-------------------------------|---|-------------------------------------|--|
| Poly(3,4-ethylenedioxythiophene) (PEDOT)/Manganese Dioxide (MnO ₂) Micromotor | Tubular | 5 μm (Diameter) 15 μm (Length) (SEM) 23 ± 4.4 | H ₂ O ₂ | Template Electrodeposition | - | <i>Small</i> , 2020 , 2003678. |
| Pot-like Structure Pt Motors. | Pot-like | μm (Diameter) (SEM) | H ₂ O ₂ | Physical Vapor Deposition/ Colloidal Chemistry Method | - | <i>Nanoscale</i> , 2014 , 6, 11177–11180. |
| Pt Micromotors | Pot-like (Rough) | ~3 μm (Diameter) (SEM) 550~700 | H ₂ O ₂ | Physical Vapor Deposition/ Colloidal Chemistry Method | - | <i>ACS Nano</i> , 2016 , 10, 8751–8759. |
| Carbonaceous Nanoflask (CNF) Motor | Flask-like | nm (Diameter) (SEM) | H ₂ O ₂ | Colloidal Chemistry Method | - | <i>Langmuir</i> , 2020 , 36, 7039–7045. |
| Pt–Polystyrene (PS) Micromotors | Dimer | ~1 μm (Diameter) (SEM) | H ₂ O ₂ | Colloidal Chemistry Method | - | <i>Langmuir</i> , 2014 , 30, 3477–3486. |
| PS–PS@Polydopamine (PDA)@Pt Micro-/Nanomotors | Dimer | ~0.2 μm to 1 μm (Diameter) (SEM and TEM) | H ₂ O ₂ | Colloidal Chemistry Method | - | This work |
| Silver (Ag) Catalytic Micromotors | Janus Particles | ~20 μm (Diameter) (SEM) | H ₂ O ₂ | Physical Vapor Deposition/ Colloidal Chemistry Method | - | <i>J. Am. Chem. Soc.</i> , 2014 , 136, 2719–2722. |
| Fe-MnO ₂ Core-shell Micromotors | Particles (Rough) | ~2 μm (Diameter) (SEM) | H ₂ O ₂ | Colloidal Chemistry Method | Decontamination of antibiotics | <i>Appl. Catal. B.</i> , 2022 , 314, 121484. |
| Cobalt-Ferrite (CFO) Micromotor | Particles | ~100 μm (Diameter) (SEM) | H ₂ O ₂ | Colloidal Chemistry Method | Removal of malachite green in water | <i>Small</i> , 2022 , 18, 2107619. |
| Hyperbranched Polyamide/L-arginine (HLA _n) Micro-/Nanomotors | Particles | ~120 nm to Several Micrometers (Diameter) (SEM and TEM) | H ₂ O ₂ | Colloidal Chemistry Method | - | <i>Nat. Commun.</i> , 2019 , 10, 966. |